Monitoring the Timing of ATP Hydrolysis with Activation of Peptide Cleavage in *Escherichia coli* Lon by Transient Kinetics†

Diana Vineyard,‡ Jessica Patterson-Ward,‡ Anthony J. Berdis,§ and Irene Lee*,‡

Department of Chemistry and Department of Pharmacology, Case Western Reserve University, Cleveland, Ohio 44106

Received June 30, 2004; Revised Manuscript Received October 14, 2004

ABSTRACT: *Escherichia coli* Lon, also known as protease La, is an oligomeric ATP-dependent protease, which functions to degrade damaged and certain short-lived regulatory proteins in the cell. To investigate the kinetic mechanism of *E. coli* Lon protease, we performed the first pre-steady-state kinetic characterization of the ATPase and peptidase activities of this enzyme. Using rapid quench-flow and fluorescence stopped-flow spectroscopy techniques, we demonstrated that ATP hydrolysis occurs before peptide cleavage, with the former reaction displaying a burst and the latter displaying a lag in product production. The detection of burst kinetics in ATP hydrolysis is indicative of a step after nucleotide hydrolysis being rate-limiting in ATPase turnover. At saturating substrate concentrations, the lag rate constant for peptide cleavage is comparable to the k_{cat} of ATPase, indicating that two hydrolytic processes are coordinated during the first enzyme turnover. The involvement of subunit interaction during enzyme catalysis was detected as positive cooperativity in the binding and hydrolysis of substrates, as well as apparent asymmetry in the ATPase activity in Lon. When our data are taken together, they are consistent with a reaction model in which ATP hydrolysis is used to generate an active enzyme form that hydrolyzes peptide.

Escherichia coli Lon, also known as protease La, is an oligomeric ATP-dependent protease, which functions to degrade damaged and certain short-lived regulatory proteins in the cell (*1*−*10*). *In vitro* this enzyme is capable of degrading polypeptides in the presence of certain nonhydrolyzable ATP analogues. However, optimal protein degradation does require ATP hydrolysis (*3*, *6*, *11*). Lon represents one of the simplest forms of ATP-dependent proteases because both the ATPase and the protease domains are located within a single monomeric subunit (*12*, *13*).

Although a complete crystal structure of active Lon has yet to be determined, some structural clues to the mechanism of Lon are available. The crystal structure of a proteolytically inactive Lon mutant lacking an ATPase domain reveals that Lon is hexameric and contains a central cavity commonly found in the ATPase and protease subunits of other ATP-dependent proteases (*14*). Additionally, the structure of the α subdomain of the ATPase subunit of Lon has been determined (*15*). This monomeric subdomain constitutes the last 25% of the carboxyl-terminal region of the ATPase domain and lacks the conserved Walker motifs found in ATP-binding proteins. On the basis of these reports, Lon appears to be structurally similar to other ATP-dependent proteases such as the bacterial homologue of the proteasome, HslUV (*16*, *17*). Whether and how ATP binding and hydrolysis are coupled to peptide cleavage are key inquiries in understanding the mechanism of the enzyme.

The coupling of ATP binding and hydrolysis to peptide cleavage is a key question in mechanistic studies of Lon protease. On the basis that ADP inhibits the ATPase and the protease activities and nonhydrolyzable ATP analogues support peptide cleavage, an ADP/ATP exchange mechanism has been proposed (*3*, *6*, *18*−*21*). However, it is not known whether peptide cleavage occurs before or after ATP hydrolysis. To evaluate the functional relationship between ATP hydrolysis and peptide cleavage, we developed a fluorescent peptide substrate whose degradation by Lon exhibits ATPase dependency as observed in the endogenous protein substrates of Lon (*11*, *22*). This defined model peptide substrate containing 10% of the fluorescent peptide Y(NO_2)-RGITCSGRQK(Abz) and 90% S2 (S3)[1] and its nonfluorescent analogue (S2) were previously used as simplified mimics of the *E. coli* Lon substrate, the λ N protein, to demonstrate that k_{cat} but not K_m of the peptide cleavage is dependent on ATP hydrolysis (*11*). In addition, the k_{cat} of peptide cleavage is higher when hydrolyzable nucleotides rather than nonhydrolyzable ATP analogues are used as activators. During peptide cleavage, the nucleotide hydrolysis activity of Lon

† This work was support by the NIH Grant GM067172.

* To whom correspondence should be addressed. Telephone: 216-368-6001. Fax: 216-368-3006. E-mail: irene.lee@case.edu.

‡ Department of Chemistry.

§ Department of Pharmacology.

[1] Abbreviations: AMPPNP, adenylyl 5-imidodiphosphate; DTT, dithiothreitol; Abz, anthranilamide; Bz, benzoic acid amide; NO_2, nitro; HBTU, *O*-benzotriazole-*N*,*N*,*N*′,*N*′-tetramethyluroniumhexafluorophosphate; Tris, 2-amino-2-(hydroxymethyl)-1,3-propanediol; HEPES, *N*-2-hydroxyethylpiperazine-*N*′-ethanesulphonic acid; $Mg(OAc)_2$, magnesium acetate; KOAc, potassium acetate; PEI−cellulose, polyethyleneimine−cellulose; λ N, also known as the λ N protein, a λ phage protein that allows *E. coli* RNA polymerase to transcribe through termination signals in the early operons of the phage; S2, a nonfluorescent analogue of S3 that is cleaved by Lon in the same manner as S3:YRGITCSGRQK(benzoic acid amide) (Bz); S3, a mixed peptide substrate containing 10% of the fluorescent peptide Y(NO_2)RGITCSGRQK(Abz) and 90% S2.

10.1021/bi048618z CCC: $30.25
Published on Web 01/11/2005

is also elevated, suggesting a coupling between the two hydrolytic activities (*23*). Because both peptides were degraded by *E. coli* Lon in an identical manner, the S3 and S2 peptide could be used as substrates to monitor the peptidase and ATPase activity of Lon, respectively (*11*).

While initial velocity and product inhibition studies identified which enzyme forms predominate under certain reaction conditions, they could not evaluate whether ATP hydrolysis precedes or follows peptide cleavage (*11*). This question, however, can be answered by measuring the rates of ATP and peptide hydrolysis in the pre-steady state. If ATP hydrolysis occurs before peptide cleavage, its rate constant should be higher than that for peptide cleavage. In this study, we utilized rapid chemical-quench-flow and fluorescence stopped-flow techniques to monitor pre-steady-state time courses of the two reactions to correlate the timing of ATP hydrolysis with peptide cleavage, thereby establishing the sequence of events occurring along the reaction pathway. In addition, despite its existence as a homooligomer, Lon exhibits two different affinities for ATP ($K_d = 10$ μM and $K_d < 1$ μM) (*19*); the mechanism by which these two kinds of ATPase sites affect proteolysis are not known. Therefore, by determining the pre-steady-state kinetics of peptide and ATP hydrolysis at low (<10 μM) versus high (100 μM) ATP concentrations, we can evaluate how the binding and/or hydrolysis of the nucleotide at the respective ATPase site coordinates with the first turnover of peptide cleavage.

MATERIALS AND METHODS

Materials. ATP was purchased from Sigma, whereas [α-^{32}P]ATP was purchased from Perkin−Elmer or ICN Biomedical. Fmoc-protected amino acids, Boc-anthranilamide (Abz), Fmoc-protected Lys Wang resin, and *O*-benzotriazole-*N*,*N*,*N*′,*N*′-tetramethyluroniumhexafluorophosphate (HBTU) were purchased from Advanced ChemTech and NovaBiochem. 2-Amino-2-(hydroxymethyl)-1,3-propanediol (Tris), *N*-2-hydroxyethylpiperazine-*N*′-ethanesulphonic acid (HEPES), and polyethyleneimine−cellulose (PEI−cellulose) TLC plates were purchased from Fisher.

General Methods. Peptide synthesis and protein purification procedures were performed as described previously (*22*). All enzyme concentrations are reported as Lon monomer concentrations. All reagents are reported as final concentrations.

Acid-Quench Peptidase Assay. Assays were performed at 37 °C and contained 50 mM Tris-HCl (pH 8.1), 5 mM magnesium acetate ($Mg(OAc)_2$), 5 mM dithiothreitol (DTT), 800 μM S3 peptide substrate (containing 50% of the fluorescent peptide, S1, and 50% S2, the nonfluorescent analogue of S1 that is degraded by Lon in an identical manner as S1), and 1 μM *E. coli* Lon monomer. The reaction was initiated by the addition of 500 μM ATP, and 10 μL aliquots were quenched with 58 μL of 0.5 N HCl at 0, 0.5, 1, 2, 3, and 5 min. After trichloroacetic acid precipitation, which removed Lon, the reaction mixtures were neutralized with 1 M Tris/2 N NaOH to pH 8 and the fluorescence (excitation of 320 nm and emission of 420 nm) of the solution was measured using a Fluoromax 3 spectrofluorimeter (Horiba Group).

Pre-steady-State Time Courses of S3 Cleavage by Fluorescent Stopped Flow. Pre-steady-state experiments were performed on a KinTek Stopped Flow controlled by the data collection software Stop Flow version 7.50 β. The sample syringes were maintained at 37 °C by a circulating water bath. Syringe A contained 5 μM Lon monomer, with variable concentrations of the peptide substrate S3 (from 5 to 500 μM), 5 mM $Mg(OAc)_2$, 50 mM Tris-HCl (pH 8.1), and 5 mM DTT. Syringe B contained varying ATP (1−500 μM). Peptide cleavage was detected by an increase in fluorescence (excitation of 320 nm and emission of 420 nm) following rapid mixing of syringe contents in the sample cell. The baseline fluorescence was normalized to zero, and the data shown are a result of averaging at least four traces. The concentration of hydrolyzed peptide was calibrated by determining the maximum fluorescence generated per micromolar peptide because of complete digestion by trypsin under identical reaction conditions in the stopped-flow apparatus. The averaged time courses were fit with eq 1

$$Y = A \exp^{-k_{lag}t} + v_{ss}t + C \quad (1)$$

where t is time in seconds, Y is the concentration of hydrolyzed peptide S3 in micromolar, A is the amplitude of the reaction, k_{lag} is the pre-steady-state rate constant in per seconds, v_{ss} is the steady-state rate in units of micromolar product per second, and C is the endpoint. The v_{ss} value can be converted to a first-order rate constant (k_{ss} in the unit of per seconds) by division with the enzyme concentration (*24*). Equation 1 is the general function that quantifies a biphasic time course. When $Y = 0$ at $t = 0$, $C = -A$ and eq 1 becomes

$$Y = -A + A \exp^{-k_{lag}t} + v_{ss}t$$

such that

$$Y = -A(1 - \exp^{-k_{lag}t}) + v_{ss}t$$

When A is defined as $v_{ss} - v_i/k_{lag}$, eq 1 becomes equivalent to the equation defining hysteresis (*25*, *26*), where v_i is the rate corresponding to the initial phase of the time course.

Data Processing. Plots displaying sigmoidal behavior were fit with eq 2 where k is the observed rate constant of the

$$k = \frac{k_{max}[S]^n}{K' + [S]^n} \quad (2)$$

reaction being monitored, k_{max} is the maximum rate constant (referred to as $k_{cat,S3}$ for $k_{ss,S3}$ data, $k_{lag,S3}$ for k_{lag} data, and $k_{cat,ATP}$ for $k_{ss,ATP}$ data), [S] is the variable substrate, K' is the Michaelis constant for S, and n is the Hill coefficient. The K_s is calculated from the relationship $\log K' = n \log K_s$, where K_s is the [S] required to obtain 50% of the maximal rate constant of the reaction. Plots displaying hyperbolic behavior, i.e., when the Hill coefficient in eq 2 becomes 1, were fit using eq 3 where k is the observed rate constant,

$$k = \frac{k_{max}[S]}{K_s + [S]} \quad (3)$$

k_{max} is the maximum rate constant (referred to as $k_{cat,S3}$ for $k_{ss,S3}$ data, $k_{lag,S3}$ for k_{lag} data, and $k_{cat,ATP}$ for $k_{ss,ATP}$ data), [S] is the variable substrate, and K_s is the [S] required to obtain 50% of the maximal rate constant of the reaction. The K_s

value was referred to as $K_{m,S3}$ when S3 hydrolysis was monitored at varying S3 concentrations. Alternatively, the K_s value was referred to as $K_{m,ATP}$ when ATP hydrolysis was monitored at varying ATP concentrations.

Chemical-Quench ATPase Activity Assays. The pre-steady-state time courses for ATP hydrolysis were measured using a rapid chemical-quench-flow instrument from KinTek Corporation. All solutions were made in 50 mM HEPES buffer at pH 8.1, 5 mM DTT, 5 mM $Mg(OAc)_2$, and 75 mM potassium acetate (KOAc). A 15 μL buffered solution of 5 μM Lon monomer, with and without 500 μM S2 or 10 μM casein, was rapidly mixed with a 15 μL buffered solution of ATP containing 0.01% of [α-^{32}P]ATP at 37 °C for varying times (0−3 s) before quenching with 0.5 N formic acid and then extracted with 200 μL of phenol/chloroform/isoamyl alcohol at pH 6.7 (25:24:1). A 3 μL aliquot of the aqueous solution was spotted directly onto a PEI−cellulose TLC plate (10 × 20 cm), and the plate was developed in 0.75 M potassium phosphate buffer (pH 3.4) to separate ADP from ATP. The relative amount of radiolabeled ADP and ATP at each time point was quantified by a Cyclone Phosphor imager (Perkin−Elmer Life Science). To compensate for the slight variations in spotting volume, the concentration of the ADP product obtained at each time point was corrected for using an internal reference as shown in eq 4. All assays were

$$[\mathrm{ADP}] = \left(\frac{\mathrm{ADP_{dlu}}}{\mathrm{ATP_{dlu}} + \mathrm{ADP_{dlu}}}\right)[\mathrm{ATP}] \qquad (4)$$

performed at least 3 times, and the average of those traces was used for data analysis. The burst amplitudes and burst rates were determined by fitting the k_{obs} data from 0 to 400 ms with eq 5. where t is time in seconds, Y is [ADP] in

$$Y = A \exp^{-k_{burst}t} + C \qquad (5)$$

micromolar, A is the burst amplitude in micromolar, k_{burst} is the burst rate constant in per seconds, and C is the end point. The observed steady-state rate constants ($k_{ss,ATP}$) were determined by fitting the data from 600 ms to 1.8 s with the linear function, $Y = mX + C$, where X is time, Y is [ADP]/[E], m is the observed steady-state rate constant in per seconds, and C is the y intercept. Data fitting was accomplished using the nonlinear regression program KaleidaGraph (Synergy).

Pulse-Chase ATPase Activity Assays. The pre-steady-state time courses of ATP hydrolysis were also measured using a pulse-chase experiment on the rapid quench. Lon (±0.5 mM S2) was rapidly mixed with radiolabeled ATP at 37 °C for 0−1.8 s, followed by a 10 mM unlabeled ATP chase for 60 s before quenching with 0.5 N formic acid. The amount of ADP produced at each time point was quantified as described in the chemical-quench assay (see above). The burst amplitude (A) and burst rate constant (k_{burst}) were determined from the time courses by fitting the data from 0 to 400 ms with eq 5.

Filter Binding Assay. A total of 2−5 μL of a 35 μM stock of Lon was incubated with 10 μM [α-^{32}P]ATP in 30 μL of 50 mM HEPES at pH 8.1, 5 mM $Mg(OAc)_2$, 75 mM KOAc, and 2 mM DTT at 37 °C for 20 min to convert all ATP to ADP. The reactions were then chilled on ice, and 3 μL of the reactions (performed 3 times) was spotted onto a piece of nitrocellulose mounted onto a dot-blot apparatus (BioRad)

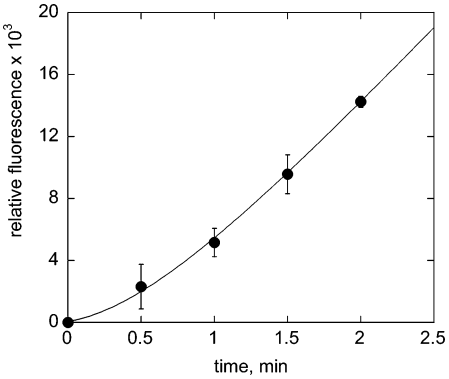

FIGURE 1: Detection of ATP-dependent S3 cleavage by a discontinuous acid-quench assay. Lon (1 μM monomer) was incubated with 800 μM S3, and reaction aliquots were quenched at the indicated times. The fluorescence signals associated with peptide cleavage were measured and plotted against their corresponding reaction time points. The experiment was performed 2 times, and the averaged data were plotted. The data were fit with eq 1 to yield a lag rate constant of 1.4 s^{-1}.

as described by Gilbert and Mackey (*24*). Each spot was washed with 10 μL of cold buffer and dried under vacuum for 30 min. In the absence of vacuum, the nitrocellulose was spotted with 2 μL of each reaction and then air-dried. The radioactive counts at each spot were quantified by PhosphorImaging.

RESULTS

Pre-Steady-State Kinetic Analysis of S3 Cleavage. Previously, we demonstrated that the pre-steady-state time course of S3 cleavage could be monitored by stopped-flow fluorescence spectroscopy (*11*). Using ATP as the activator, we detected lag kinetics in S3 cleavage. The lag phase is lengthened by 7-fold when adenylyl 5-imidodiphosphate (AMPPNP), a non-hydrolyzable ATP analogue, was used as an activator. Because the cleavage of S3 peptide generates a fluorescent signal as a result of the separation of the fluorescent quencher, 3-nitrotyrosine, from the fluorescent donor, anthranylamide, the lag in S3 cleavage could be attributed to a slow step prior to peptide bond cleavage or to the slow dissociation of the donor from the quencher because both hydrolyzed peptides remain bound to the active site of the enzyme. To determine if slow dissociation of peptide products caused the lag, we monitored the time course of 800 μM S3 cleavage by 1 μM monomeric Lon using a discontinuous acid-quench assay. An aliquot of the reaction was quenched with HCl at the times indicated in Figure 1, and the fluorescence intensity at each time point was measured to yield the time course for S3 cleavage. Despite acid denaturation that released hydrolyzed peptides from Lon, the lag phase remained in the fluorescence time course of S3 cleavage. This result indicates that the separation of the hydrolyzed peptide from Lon does not contribute to the observed lag phase of the reaction. Furthermore, a lag rate constant of 1.4 ± 0.6 s^{-1} was obtained by fitting the data with eq 1, which is a general function used to determine the rate constant (k) associated with a single-exponential phase followed by a steady-state phase, and is related to the hysteresis equation as described in the Materials and Methods. This observed value is 2-fold higher than that obtained previously using stopped-flow spectroscopy (*11*) and may be attributed to a difference in the detection methods

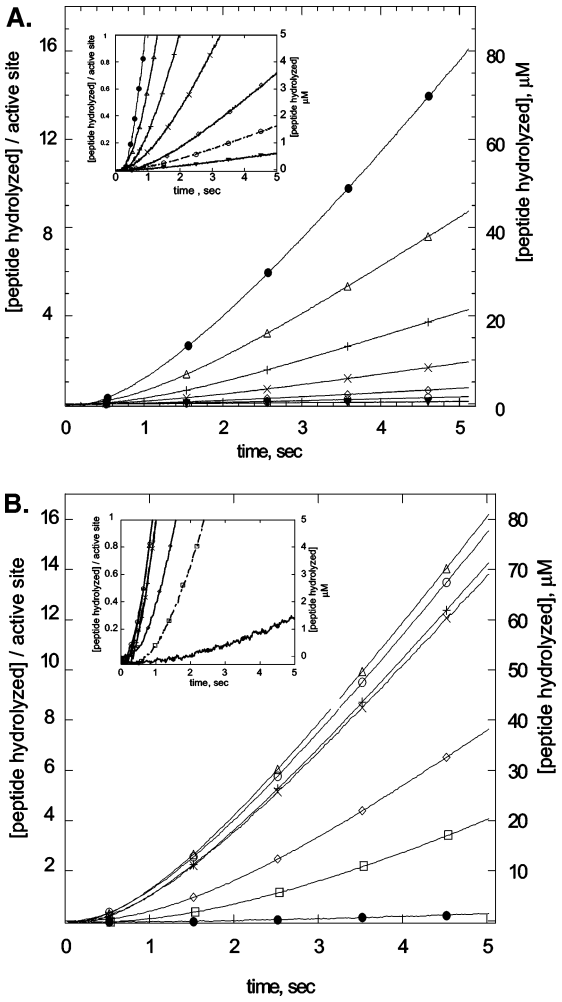

FIGURE 2: Stopped-flow analysis of ATP-dependent S3 cleavage by *E. coli* Lon. (A) ATP (500 μM) was incubated with 5 μM monomeric Lon in the presence of 5 (▼), 10 (○), 25 (◇), 50 (×), 100 (+), 200 (△), and 500 (●) μM S3. The inset zooms in A to show the lag for one peptide hydrolyzed per active site. The fluorescence changes associated with peptide cleavage were converted to product concentrations as described in the Materials and Methods. Each time course shown is an average of 4 traces. The values on the right *y* axis represent the concentration of peptide hydrolyzed, whereas the values on the left *y* axis represent the mole equivalent of peptide digested by each Lon monomer. (B) S3 (500 μM) was digested by 5 μM Lon monomer in the presence of 1 (●), 5 (□), 10 (◇), 50 (×), 100 (+), 200 (△), and 500 (○) μM ATP. The inset zooms in B to show the lag for one peptide hydrolyzed per active site. Each time course shown is an average of at least 4 traces. The right *y* axis shows the amount of peptide hydrolyzed, whereas the left *x* axis shows the mole equivalent of peptide cleavage by each Lon monomer.

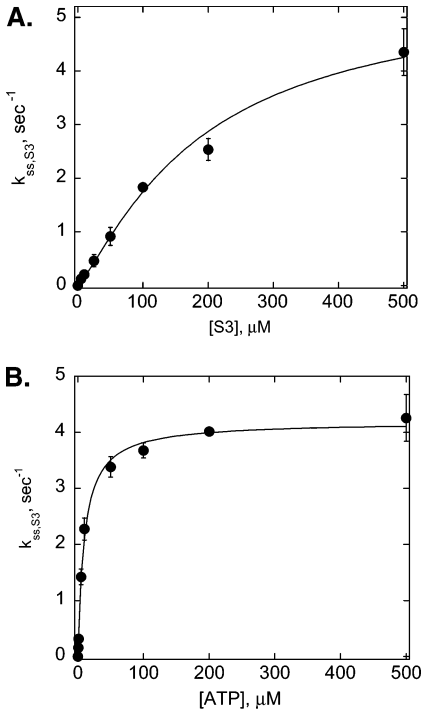

FIGURE 3: Steady-state kinetics of ATP-dependent S3 cleavage by 5 μM *E. coli* Lon monomer. The $k_{ss,S3}$ values were obtained by dividing the steady-state rates of the reactions by [Lon] as described in the Materials and Methods. (A) Steady-state rates of S3 cleavage (v_{ss}) were obtained by fitting the stopped-flow time courses of peptide cleavage at varying [S3] with eq 1 (Materials and Methods). The data presented in this plot were best-fit with eq 2, and the kinetic parameters obtained were $k_{cat,S3} = 5.5 \pm 0.8$ s^{-1}, $K_{m,S3} = 188 \pm 148$ μM, and $n = 1.23 \pm 0.2$ as summarized in Table 1. (B) Steady-state rates of S3 cleavage (v_{ss}) were obtained by fitting the stopped flow-time courses of peptide cleavage at varying [ATP] with eq 1 (Materials and Methods). The data presented in this plot were best-fit with eq 3, and the kinetic data obtained from the fit were $k_{cat,S3} = 4.2 \pm 0.1$ s^{-1} and $K_{ATP} = 9.7 \pm 0.9$ μM as summarized in Table 1.

(a continuous versus discontinuous assay). Despite the slight variation in the lag rate constants, both the stopped-flow and the acid-quenched reactions displayed lag kinetics, indicating that the dissociation of the peptide products from Lon did not contribute to the lag phase.

To determine the stoichiometry of S3 cleavage, we generated a calibration curve by measuring the fluorescence changes associated with the complete degradation of known concentrations of S3 by trypsin in a stopped-flow apparatus. This technique allows us to accurately define the amount of peptide cleaved during the time courses for S3 cleavage. Experiments were performed at 500 μM ATP with several fixed levels of S3 (5−500 μM, Figure 2A) as well as a fixed concentration of S3 (500 μM) and several fixed levels of ATP (1−500 μM, Figure 2B). As shown in parts A and B of Figure 2, a lag in peptide hydrolysis was observed in all of the time courses. The lag rate constants (k_{lag}) and the observed steady-state rate constants of peptide cleavage ($k_{ss,S3}$) were obtained by fitting each time course with eq 1. The plots of $k_{ss,S3}$ as a function of S3 and ATP concentrations are shown in parts A and B of Figure 3, and the data were fit with eqs 2 and 3, respectively, to yield the $k_{cat,S3}$ (the maximum rate constant for peptide cleavage), K_{mS3}, K_{ATP}, and Hill coefficients (n) as summarized in Table 1. The steady-state kinetic parameters determined from this study (using 5 μM enzyme monomer) agree well with those determined previously at 125 nM Lon monomer ($k_{cat,S3} = 7.7$ s^{-1}; $K_{mS3} = 85$ μM, and $K_{ATP} = 7.2$ μM) (*11*), indicating that these kinetic parameters are independent of the enzyme concentration under the conditions examined. Because pre-steady-state lag kinetics could be attributed to the binding of substrates at low concentrations being rate-limiting, we measured the k_{lag} of S3 cleavage at increasing peptide or ATP concentrations. As shown in parts A and B of Figure 4, the dependence of k_{lag} toward S3 and ATP concentrations reaches saturation with a maximum $k_{lag,S3}$ value. The data were best-fit with eqs 2 and 3, respectively, to yield the kinetic parameters $k_{lag,S3}$, K_{S3}, and K_{ATP} as summarized in

Table 1: Parameters Obtained from Pre-steady-State Kinetic Characterization of ATP-Dependent S3 Cleavage by *E. coli* Lon

	0.5 mM ATP vary [S3]	0.5 mM S3 vary [ATP]
$k_{cat,S3}$	5.5 ± 0.8 s^{-1} [a]	4.2 ± 0.1 s^{-1} [b]
$K_{m,S3}$	188 ± 148 μM [a]	NA
n	1.23 ± 0.2 [a] (1.7 ± 0.2) [c]	NA
$k_{lag,S3}$	0.88 ± 0.07 s^{-1} [c]	1.14 ± 0.06 s^{-1} [d]
K_{S3}	67 ± 34 μM [c]	NA
K_{ATP}	NA	9.7 ± 0.9 [b] μM (7.2 ± 1.9 μM) [c]

[a] These values were obtained by fitting the steady-state kinetic data shown in Figure 3A with eq 2. [b] These values were obtained by fitting the steady-state kinetic data shown in Figure 3B with eq 3. [c] These values were obtained by fitting the lag rate constants obtained from the stopped-flow time courses of S3 cleavage shown in Figure 4A with eq 2. [d] NA = not available.

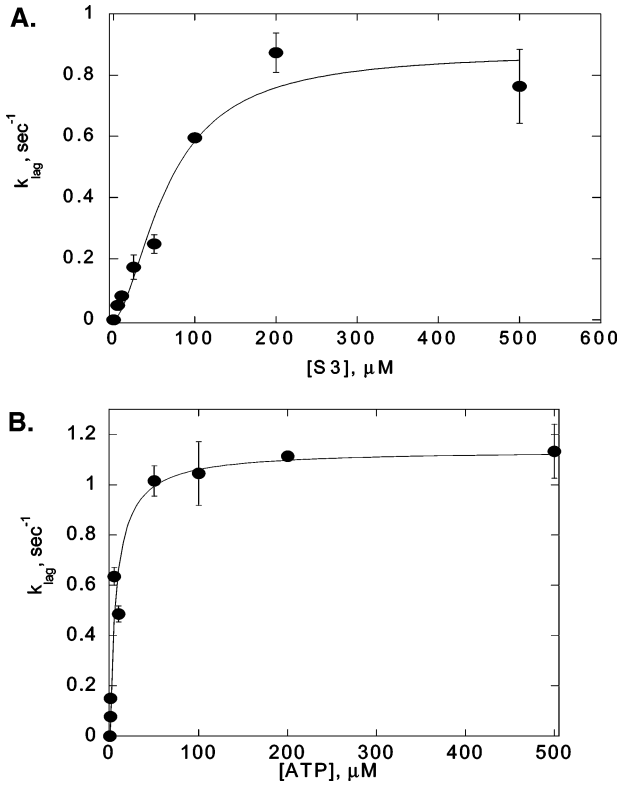

FIGURE 4: Substrate dependency of the lag rate constants of S3 cleavage. (A) Lag rate constant for S3 peptide degradation by 5 μM monomeric Lon at varying S3 was determined by fitting the stopped-flow time courses of peptide cleavage as shown in Figure 2A with eq 1. The data were collectively fit with eq 3 to yield a maximal $k_{lag,S3} = 0.88$ s^{-1}, $K_{S3} = 67$ μM, and $n = 1.7 \pm 0.2$. The error bars represent the experimental deviations among the different trials. Each data point was obtained from the average of three independent experiments, with each experiment containing at least four stopped-flow traces. (B) Lag rate constant for S3 peptide degradation by 5 μM monomeric Lon at varying ATP was determined by fitting the stopped-flow time courses of peptide cleavage as shown in Figure 2B with eq 1. The data were collectively fit with eq 2 to yield a maximal $k_{lag,S3} = 1.14$ s^{-1} and a $K_{ATP} = 7.2 \pm 1.9$ μM. The error bars represent the experimental deviations among the different trials. Each data point was obtained from the average of three independent experiments, with each experiment containing at least four stopped-flow traces.

Table 1. The maximum lag rate constant for S3 cleavage ($k_{lag,S3}$), determined at varying S3 and varying ATP concentrations, was 0.88 ± 0.07 and 1.14 ± 0.06 s^{-1}, respectively. These values are in close agreement with the lag rate constant of 0.76 s^{-1} determined previously by fitting the fluorescent time courses with the hysteresis equation (*11*), which is a specific form of eq 1 (see the Materials and Methods) used to characterize enzymes responding slowly to a change in the ligand concentration (*25*, *26*). At high S3 or ATP concentrations, substrate binding no longer limits the rate of the first peptidase turnover, and thus, the maximum $k_{lag,S3}$ value directly reflects the rate constant for the build-up of at least one reaction intermediate that leads to peptide hydrolysis at the active site of the enzyme. Furthermore, the fit of the $k_{lag,S3}$ dependence on S3 or ATP concentrations to eq 2 (for S3) or eq 3 (for ATP) provided the apparent K_d values of the respective substrate (K_{S3} and K_{ATP} in Table 1). The K_{S3} value (67 ± 34 μM) is comparable to the K_m of S3 cleavage (188 ± 148 μM), whereas K_{ATP} (9.7 ± 0.9 μM) is in close agreement with the weak affinity ATPase site in *E. coli* Lon, which is 10 μM (*17*).

Chemical-Quench Analysis of ATP Hydrolysis. Because the k_{cat} of S3 cleavage is enhanced by nucleotide hydrolysis (*11*, *21*) and the k_{cat} of ATP hydrolysis is stimulated by the peptide or protein substrate (*3*, *21*, *23*), it is very likely that the two hydrolytic processes are coupled through a common enzyme intermediate. To begin identifying such an intermediate, we measured the time courses of the first turnover of ATP hydrolysis in the absence and presence of the peptide or protein substrate using the rapid chemical-quench technique. Lon (5 μM monomer) was preincubated with 500 μM S2, the nonfluorescent analogue of S3 that was degraded by Lon identically as S3 (5× K_{mS3}, Table 1, see ref *11*), and rapidly mixed with 100 μM ATP (10× K_{ATP}, Table 1) prior to quenching with formic acid at times between 0 and 3 s. The time courses for ATP hydrolysis measured in the absence and presence of casein (protein substrate) were also determined (Figure 5A) for comparison. All three time courses showed an identical burst in ADP production within the first 200 ms of the reaction, followed by at least one slower phase in product formation. The detection of a pre-steady state burst in the acid-quench experiments is indicative of the rate-limiting step occurring after ATP hydrolysis. Although the S2 peptide is smaller than casein and contains only one Lon cleavage site, it stimulates ATP hydrolysis like the protein substrate, thereby indicating that both substrates share identical mechanisms in ATPase stimulation. The data in Figure 5A were initially fit with eq 1 (with k_{lag} becoming k_{burst}), which characterizes a single-exponential burst phase followed by a linear steady-state turnover rate of the reaction. As shown in Figure 5B and the inset, the data obtained during the first 400 ms of the time courses showed a poor fit with eq 1 and the burst amplitudes were also significantly underestimated. To better evaluate the burst amplitudes as well as the burst rates of the reactions, we fit the data within the first 400 ms of the time courses, which consisted of a burst and a relatively constant transition phase in ADP formation, with eq 5 to yield the values summarized in Table 2. As shown in Table 2 and parts A and C of Figure 5, the burst amplitudes as well as the burst rate constants for the three time courses are comparable but the steady-state rates of the intrinsic versus stimulated ATPase reactions differ. The steady-state phase of the time courses (from 600 ms to 1.8 s) were fit with a linear function to yield the steady-state turnover numbers of 0.23 ± 0.02, 0.69 ± 0.01, and 0.67 ± 0.03 s^{-1}, corresponding to the intrinsic, S2-stimulated,

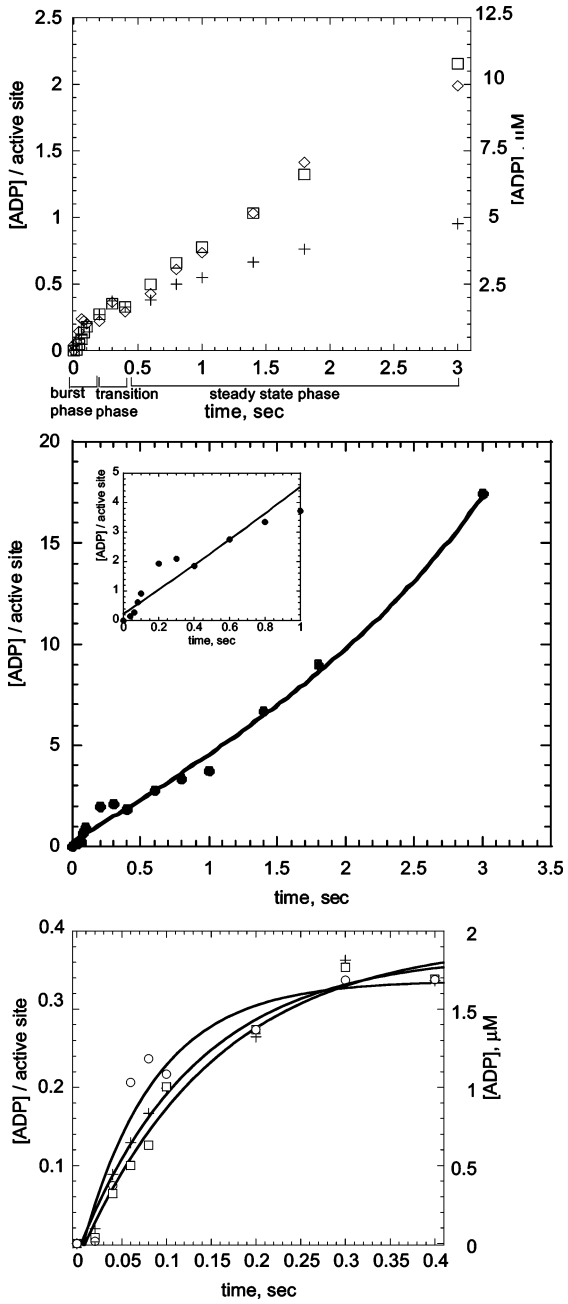

FIGURE 5: Pre-steady time courses of ATP hydrolysis by *E. coli* Lon. (A) [α-^{32}P]ATP (100 μM) was incubated with 5 μM monomeric Lon in the absence (+) and presence of 500 μM S2 (□) or 10 μM casein (◇), and the reactions were quenched with acid at the indicated times. The concentrations of [α-^{32}P]ADP generated in the reactions were determined by TLC followed by PhosphorImaging as described in the Materials and Methods. The values on the *y* axis were obtained by dividing [ADP] produced by 5 μM Lon, which reflects the mole equivalent of ADP produced per Lon monomer. (B) [α-^{32}P]ATP (200 μM) was incubated with 5 μM monomeric Lon in the presence of 500 μM S2. The time points were obtained by quenching the reactions with acid at the indicated times, and the resulting time course for ADP production was fit with the equation $Y = A\exp(-k_{obs}t) + v_{ss}t + C$, where A is the burst amplitude, k_{obs} is the observed burst rate constant, v_{ss} is the steady-state rate, and C is the endpoint. The inset shows the fit of the data spanning 0−400 ms. (C) Time points from 0 to 400 ms were fit with eq 5 (Materials and Methods) to yield burst amplitudes for intrinsic, casein-stimulated, and S2-stimulated time courses of 1.92 ± 0.12, 1.8 ± 0.2, and 2.06 ± 0.15 μM, respectively, as summarized in Table 2. The burst rate constants were 7.6 ± 1.3, 12.2 ± 3.2, and 6.5 ± 1.4 s^{-1}, respectively, which are also summarized in Table 2.

and casein-stimulated ATPase reactions, respectively. Despite the inclusion of 5 μM monomeric Lon in the reactions however, only ~2 μM burst of ADP production was detected in all three time courses, suggesting that only 40% of the Lon monomer hydrolyzes ATP during the first enzyme turnover.

Comparison of ATPase and S3 Cleavage. To assess how ATP hydrolysis and peptide cleavage are kinetically coordinated, we compared the time courses of peptide cleavage and peptide-stimulated ATP hydrolysis under identical reaction conditions as shown in Figure 6 (5 μM Lon monomer, 100 μM ATP, and 500 μM peptide). The pre-steady-state phase of ATP hydrolysis consists of the burst of ADP production ($k_{burst,ATP} = 6.5 \pm 1.4\ s^{-1}$) and the transition phase, which together spans the first 400 ms of the reaction. Steady-state turnover of ATP hydrolysis, which reflects mostly the rate-limiting step of the reaction, occurs thereafter with a turnover number of 0.69 ± 0.01 s^{-1}. Under identical reaction conditions, the lag in S3 cleavage persists for approximately 1 s with a lag rate constant of 0.94 ± 0.08 s^{-1} prior to the attainment of steady-state turnover in S3 cleavage at 3.7 ± 0.2 s^{-1}. The close agreement between the lag rate constant for peptide hydrolysis and the k_{cat} of peptide-stimulated ATPase suggests that the first turnover of peptide cleavage may be coupled with the rate-limiting step of peptide-stimulated ATPase activity.

As indicated in the above experiments, despite the inclusion of 5 μM Lon monomer in the ATPase reactions, only 2 μM ADP formation were detected in the burst phases of the ATPase time course. Because the acid-quench experiments measured ADP formation at the active site of the enzyme, the detection of a substoichiometric burst could be attributed to 40% of the enzyme saturated with ATP because of the low nucleotide concentration. If this explanation is correct, the burst amplitude, which reflects the active ATPase concentration, should increase with the nucleotide concentration. To test this hypothesis, we monitored the ATPase reaction in the presence of 5 μM Lon monomer, 500 μM S2, and varying [ATP] for 1.8 s. Figure 7 shows that the time courses display triphasic behavior as discussed above in Figure 5A. The steady-state rates of ATP hydrolysis were obtained by fitting the data from 600 ms to 1.8 s with a linear function. Plotting the observed steady-state rate constants of ATPase ($k_{ss,ATP}$) versus the ATP concentration yields Figure 8A, which was best fit with eq 2. The $k_{cat,ATP}$ value determined from this analysis was 1.4 ± 0.1 s^{-1}, and the $K_{m,ATP}$ was 76 ± 33 μM, both of which closely agree with that of 1 s^{-1} and 49 μM determined previously at 150 nM monomeric Lon (*23*). The Hill coefficient obtained from the fit of these data was 1.7 ± 0.2. Although *E. coli* Lon exists predominantly as a homooligomer, it exhibits at least two different affinities for ATP (K_d < 1 μM and K_d = 10 μM) (*19*). Because each monomeric subunit contains only one ATP-binding site, it is conceivable that the ATPase sites in oligomeric Lon are asymmetrical in their functions. Therefore, the detection of a Hill coefficient close to 2 could be a measurement of the communication between two functionally nonequivalent subunits during enzyme catalysis. This speculation however, will require further evaluation by biophysical approaches that relate the oligomeric state of Lon with enzymatic activities.

Table 2: Parameters Obtained from Pre-steady-State Kinetic Characterization of the ATPase Activity of *E. coli* Lon

	intrinsic ATPase	+20 μM casein	+500 μM S2
$k_{cat,ATP}$	NA	NA	1.4 ± 0.1 s^{-1} [a]
$K_{m,ATP}$	NA	NA	76 ± 33 μM[a]
n	NA	NA	1.7 ± 0.2[a] (1.4 ± 0.1)[b]
K_{ATP}	NA	NA	22 ± 16 μM[b]
k_{burst}	7.6 ± 1.3 s^{-1} [c]	12.2 ± 3.2 s^{-1} [c]	6.5 ± 1.4[c] (11.3 ± 3.3)[a] (18 ± 2) sec^{-1} [d]
burst amplitude	1.92 ± 0.12 μM[c]	1.8 ± 0.2 μM[c]	2.06 ± 0.15[c] (2.2 ± 0.1)[b] (4.1 ± 0.1) μM[d]

[a] These values were obtained by fitting the data in Figure 8A with eq 2. [b] These values were obtained by fitting the data in Figure 8B with eq 2. [c] These values were obtained by fitting the acid-quenched time courses (0−400 ms) of ATP hydrolysis that are shown in Figure 5C with eq 5. [d] These values were obtained by fitting the pulse-chase data in Figure 10 with eq 5.

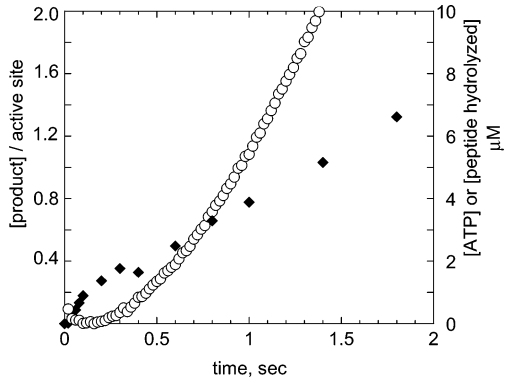

FIGURE 6: Pre-steady-state time courses for ATP hydrolysis and S3 degradation at identical reaction conditions. Monomeric Lon (5 μM) was incubated with 100 μM ATP and 500 μM peptide substrate. The time course for peptide hydrolysis (○) was determined by fluorescence stopped-flow spectroscopy using 100 μM nonradiolabeled ATP and 500 μM S3 as the substrates. The time course for ATP hydrolysis (◆) was determined by rapid acid quenching of a reaction containing Lon, 100 μM [α-^{32}P]ATP, and 500 μM S2 as described in the Materials and Methods. The values on the left *y* axis were obtained by dividing the concentrations of the peptide or ATP hydrolyzed by 5 μM Lon, whereas the right *y* axis reports the concentrations of products formed.

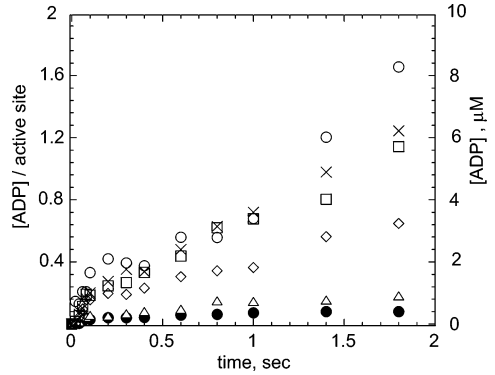

FIGURE 7: Pre-steady-state time courses at varying [ATP] and constant S2. Monomeric Lon (5 μM) was incubated with 500 μM S2 and 5 (△), 10 (●), 25 (◇), 50 (□), 100 (×), and 200 (○) μM [α-^{32}P]ATP. The reactions were rapidly quenched with acid at the indicated times, and the amount of [α-^{32}P]ADP formed was determined by PhosphorImaging. Each time course was repeated at least 3 times, and the averaged data are reported.

The burst amplitudes and burst rate constants were obtained by fitting the data spanning 0−400 ms in Figure 7 with eq 5 and plotting the respective parameters against their specific ATP concentration (parts B and C of Figure 8). Because the burst amplitude directly reflects the amount of ADP production at the active site of the enzyme, the fit of the data in Figure 8B with eq 2 provided a measurement of the apparent K_d for ATP (K_{ATP}). As shown in Figure 8B, the burst amplitudes for ATP hydrolysis exhibit a dependency on the ATP concentration and a maximum burst amplitude of 2.2 ± 0.1 μM (44% of the concentration of Lon monomer present), a K_{ATP} of 22 ± 16 μM, and a Hill coefficient of 1.4 ± 0.10 were obtained through fitting the data with eq 2. According to Figure 8C, the burst rates of ATP hydrolysis are independent of the nucleotide concentrations (5−200 μM) and the averaged burst rate constant (k_{burst}) is 11.3 ± 3.3 s^{-1}. At 5 μM ATP, it is anticipated that the tight but not the weak nucleotide-binding sites of Lon will be saturated with ATP. Therefore, the apparent independence of k_{burst} toward the indicated ATP concentrations is likely attributed to ATP hydrolysis occurring at the high-affinity sites. When our data are taken together with the observed 44% burst amplitude, they suggest that the pre-steady-state burst in ATP hydrolysis occurs at the high-affinity sites (~50% of the total monomer concentration) but the hydrolysis of ATP is coordinated with ATP binding at the low-affinity sites.

Characterization of ATP Binding. The substoichiometric burst in ADP production could be caused by either inefficient nucleotide binding or reflects the coordinated ATP binding and hydrolysis between the nonequivalent ATPase sites in Lon. To further evaluate these potential mechanisms, we measured the concentration of functional nucleotide-binding and hydrolysis sites using a filter binding assay and a pulse-chase experiment, respectively.

In the filter binding assay, several aliquots of an enzyme stock of Lon, whose concentration was predetermined by the Bradford assay (final enzyme concentration ≤ 5 μM), were incubated with 10 μM [α-^{32}P]ATP at 37 °C to yield [α-^{32}P]ADP that remained tightly bound to Lon. Because ADP competes with ATP for the same binding site and its K_i is 0.3 μM (*11*), it is anticipated that the concentration of active Lon could be defined by the population of enzyme that bound [α-^{32}P]ADP and was retained as radiolabeled protein onto the nitrocellulose. As such, the concentration of active Lon could be determined from the radioactive counts of standards containing known ATP concentrations. A plot of [^{32}P]ADP versus the volume of Lon stock added in the binding reaction yielded a linear plot (Figure 9), indicating that the concentration of Lon/[^{32}P]ADP formed was directly proportional to the amount of enzyme present in the reaction. The concentration of active Lon was calculated from the slope of the fit, which corresponds to 36 μM monomeric enzyme. This value agrees closely with the concentration of the enzyme stock determined by the Bradford assay (35 μM) and indicates that all of the monomeric Lon used in the ATPase reactions could bind the nucleotide.

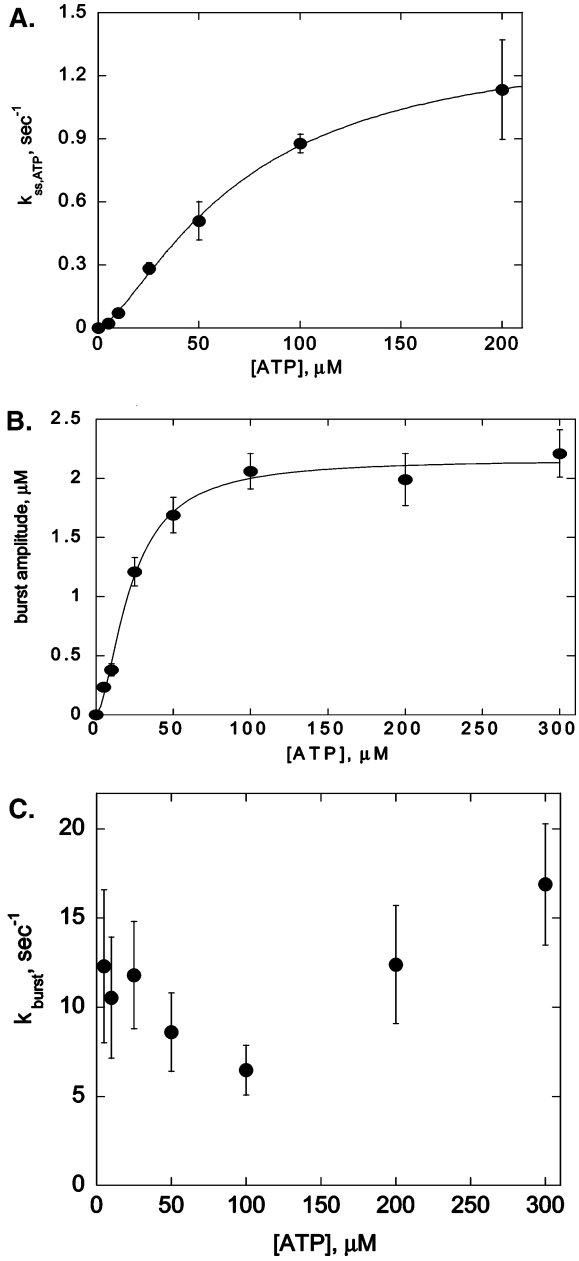

FIGURE 8: Fitting the pre-steady-state kinetic parameters of ATP hydrolysis by Lon. (A) Data from 600 ms to 1.8 s in Figure 7 were fit with a linear function to provide the steady-state rates of ATP hydrolysis at varying [ATP]. Each time point was performed at least 3 times, and the averaged data were reported. The error bars represent the error of the fit for each data point. The $k_{ss,ATP}$ values were obtained by dividing the steady-state rates by [Lon]. Plotting the $k_{ss,ATP}$ values against its specific [ATP] yields a sigmoidal plot that is best fit with eq 2. The kinetic parameters obtained from the fit were $k_{cat,ATP} = 1.4 \pm 0.1$ s^{-1}, $K_{m,ATP} = 76 \pm 33$ μM, and $n = 1.7 \pm 0.2$ and are summarized in Table 2. (B) Burst amplitudes were determined by fitting the data from 0 to 400 ms in Figure 7 with eq 5. As summarized in Table 2, the maximum burst amplitude obtained from the fit was 2.2 μM, which corresponds to ~44% of the enzyme present in the reaction, a $K_{ATP} = 22 \pm 16$ μM, and $n = 1.4 \pm 0.1$. The time points reported here are averaged values of three different trials. The error bars represent the standard error of the fit for evaluating the respective burst amplitude values at the specific [ATP]. (C) The burst rates of ATP hydrolysis were determined by the same manner as in B, and the average $k_{burst} = 11.3 \pm 3.3$ s^{-1}.

To determine if all of the monomeric Lon prepared for this study could hydrolyze ATP, we performed a pulse-chase

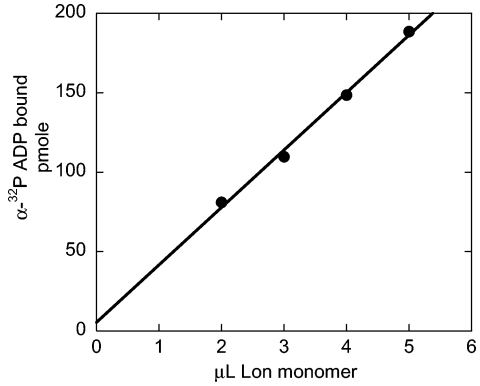

FIGURE 9: Determining the concentration of active Lon by filter binding assay. Total of 2, 3, 4, and 5 μL of a Lon stock (35 μM monomer as determined by the Bradford assay) was incubated with 10 μM [α-^{32}P]ATP at 37 °C for 20 min to convert ATP to ADP. The amount of Lon/[α-^{32}P]ADP formed in each reaction was determined by the filter binding assay described in the Materials and Methods. Plotting the amount of [α-^{32}P]ADP bound to Lon against the volume of enzyme stock added yields a straight line that was fit with the linear equation $y = mx + c$, where m equals 36 pmol of ADP/μL of Lon (36 μM Lon momomer).

experiment. In this experiment, 5 μM Lon monomer was incubated with 500 μM S2 and rapidly mixed with 100 μM [α-^{32}P]ATP as in the chemical-quench-flow experiment, except that the mixed reaction was chased with 10 mM unlabeled Mg·ATP for 60 s before quenching with acid and denaturation with phenol/chloroform. During ATP hydrolysis, [α-^{32}P]ATP bound to Lon could either be hydrolyzed to yield [α-^{32}P]ADP or dissociate from the enzyme. In the presence of 10 mM unlabeled ATP (100-fold excess over labeled ATP), any enzyme not bound to [α-^{32}P]ATP would be sequestered by the unlabeled ATP and not be detected in the assay. In the acid-quench experiment, any [α-^{32}P]ATP that bound to Lon but was not hydrolyzed remained as unreacted ATP. In contrast, the 60 s delay in the pulse-chase experiment allowed time for the enzyme to hydrolyze any [α-^{32}P]ATP that was bound during the various incubation times, and the presence of 10 mM unlabeled ATP (100-fold excess over labeled ATP) allowed for the complete exchange of [α-^{32}P]ADP for unlabeled ATP.

Figure 10 compares the time courses of ATP hydrolysis by Lon under the acid-quench and pulse-chase conditions. The data spanning the first 400 ms were fit with eq 5 to yield the burst amplitudes and k_{burst} of the respective reactions. In the presence of ATP chase, the burst amplitude was 4.1 ± *0.1* μM, which was approximately 80% of the total monomeric Lon present in the reaction. The burst rate of the chased reaction was 18 ± 2 s^{-1}, which was 2-fold higher than that determined for the chemical-quench condition under identical labeled ATP conditions. The pulse-chase result showed that at least 80% of the Lon monomer could bind and hydrolyze ATP. Therefore, the detection of a reduced burst in ADP production in the chemical-quench-flow time course was not due to the presence of inactive enzyme in the reaction. Moreover, the ATPase sites of Lon appeared to be functionally nonequivalent, because ~50% of the sites (tight affinity) hydrolyzed ATP within the first 400 ms of the reaction, whereas the remaining sites (weak affinity) hydrolyzed ATP at a much slower rate.

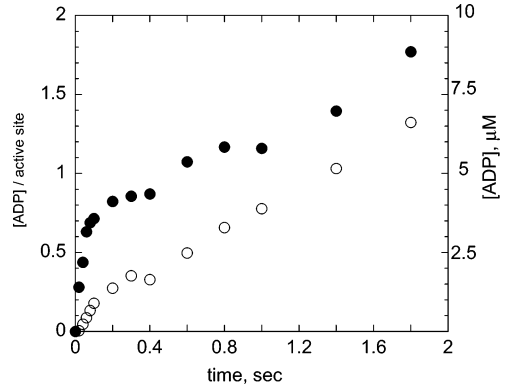

FIGURE 10: Monomeric Lon (5 μM) was incubated with 500 μM S2 and 100 μM [α-^{32}P]ATP for the indicated times and then quenched with acid (○) or chased with 10 mM Mg·ATP for 60 s prior to quenching with acid (●). The data from 0 to 400 ms were best-fit with eq 5 to yield a burst amplitude of 2.06 ± 0.15 μM and a k_{burst} of 6.2 ± 1.4 s^{-1} for the acid-quench experiment. Similarly, a burst amplitude of 4.1 ± 0.1 μM and a k_{burst} of 18 ± 2 s^{-1} were yielded for the pulse-chase experiment. The amount of [α-^{32}P]ADP generated at each time point was reported on the right *y* axis. The values on the left *y* axis were obtained by dividing the concentrations of ADP formed by 5 μM Lon.

DISCUSSION

Lon is an ATP-dependent protease functioning to degrade damaged and certain regulatory proteins *in vivo*. In this study, we demonstrated that in *E. coli* Lon, peptide cleavage is driven by ATP hydrolysis, which is coordinated with ATP binding to the low-affinity sites in the oligomeric enzyme. Our findings are in discord with the previous proposal that peptide cleavage occurs before ATP hydrolysis in Lon catalysis (*3*, *4*, *6*, *21*). In the previous studies, on the basis that proteins but not tetrapeptide substrates stimulate the ATPase activity of Lon, it was proposed that proteins bind to an allosteric site in Lon to promote ADP release, thereby facilitating enzyme turnover (*3*, *19*). Although it is known that ATP is the most effective activator of Lon protease, mechanistic details concerning how ATP hydrolysis is coupled with peptide bond cleavage is not available. To investigate the molecular mechanism of the ATPase-dependent peptidase activity in *E. coli* Lon, we performed the first pre-steady-state kinetic analysis on this enzyme by measuring the kinetics of the first turnover of ATP and peptide hydrolysis of a synthetic peptide substrate whose degradation by Lon exhibits the same ATP dependency as protein substrates (*22*). Because this peptide contains only one Lon cleavage site and it stimulates ATP hydrolysis, the data obtained from this study can be directly attributed to the ATPase-dependent peptidase reaction rather than polypeptide unfolding or processive peptide cleavage.

As presented in this study, *E. coli* Lon exhibits lag kinetics in the degradation of the model peptide but burst kinetics in ATP hydrolysis. During the lag in peptide cleavage, ~50% of the Lon monomer hydrolyzes ATP with a burst rate constant of 11.3 ± 3.3 s^{-1}. According to the ATPase kinetic data, the k_{cat} for peptide-stimulated ATPase is 1.4 s^{-1} (Table 2), which approximates the $k_{lag,S3}$ of S3 cleavage as summarized in Table 1 (0.88−1.14 s^{-1}). These results show that the first turnover of peptide hydrolysis requires the build up of a reaction intermediate, which coincides with the rapid hydrolysis of ATP during the first enzyme turnover. The burst in ATP hydrolysis further indicates that the rate-limiting step of the reaction occurs after nucleotide hydrolysis; therefore, it could be ADP product release. The detection of the rate-limiting step following ATP hydrolysis is consistent with the proposal that ADP release limits ATPase turnover (*3*, *19*) and is supported by our observation that both casein and S2 peptide stimulate only the steady-state turnover rate of ATP hydrolysis (Figure 5A). Collectively, these results support a reaction model in which activation of peptide hydrolysis is driven by ATP hydrolysis and the first turnover of peptide cleavage is coupled with the rate-limiting step in ATP hydrolysis.

Scheme 1[a]

$$E+A \underset{k_{-1}}{\overset{k_{+1}}{\rightleftharpoons}} EA \underset{k_{-2}}{\overset{k_{+2}}{\rightleftharpoons}} EAA \xrightarrow{k_{+3}} FPA \xrightarrow{k_{+4}} FA+P \xrightarrow{k_{+5}} FP \xrightarrow{k_{+6}} E+P$$

k_{+1}= 10 $\mu M^{-1}sec^{-1}$ k_{+3}= 8 sec^{-1}

k_{-1}= 0.1sec^{-1} k_{+4}= 0.8 sec^{-1}

k_{+2} = 0.14 $\mu M^{-1}sec^{-1}$ k_{+5}= 4 sec^{-1}

k_{-2}= 0.1 sec^{-1} k_{+6}= 20 sec^{-1}

[a] E and F are different catalytic forms of Lon along the reaction pathway.

This model indicates that ATP hydrolysis precedes peptide cleavage and is in discord with the earlier reaction model proposed for Lon, which suggests that peptide hydrolysis occurs before ATP consumption (*3*). The discrepancy between the two models could be attributed to the choice of peptide substrates used in evaluating the ATPase dependency of the reaction. Some of the earlier studies utilized peptides lacking ATPase stimulation abilities as substrates, which might have led to an underestimation of the contribution of ATP hydrolysis toward peptide-cleavage efficiency. Although S2 is significantly smaller than casein and contains only one Lon cleavage site, it exhibits the same ATPase stimulation profile as the latter (*23*). Together with the previous data indicating that the k_{cat} for peptide degradation is 7-fold higher in the presence of ATP versus AMPPNP, we conclude that this peptide is more suitable for evaluating the ATPase-dependent protease mechanism of Lon (*11*).

Pre-steady state kinetic analysis of the ATPase activity of Lon further reveals functional nonequivalency in the subunits of the enzyme, because only 50% of the ATP bound to Lon is hydrolyzed before peptide cleavage. The observed asymmetry in the ATPase activity could be attributed to the two different classes of ATP-binding sites found in *E. coli* Lon as reported by Menon and Goldberg [K_d < 1 μM and K_d ~ 10 μM (*19*, *20*)], who also observed that optimal protein degradation requires occupancy of ATP at each site. The molecular basis for such requirement, however, was not clear. On the basis of the ATPase data obtained in this study, we propose a sequential ATP hydrolysis reaction model that could account for the aforementioned observations (Scheme 1). Assuming that ~50% of the Lon subunits exhibit high affinity for ATP, these sites will be saturated at 5 μM ATP, which is the lowest concentration of ATP used in this study. Under this condition, Lon binds but does not hydrolyze ATP. As the concentration of ATP increases, the low-affinity sites become occupied with the nucleotide, which upon full

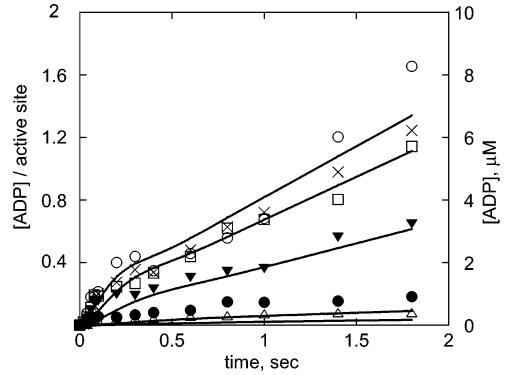

FIGURE 11: Collective fit of acid-quench ATPase data using FitSim. Simulation of the ATPase mechanism outlined in Scheme 1 was performed using FitSim. The resulting solid lines yielded a $k_{burst} = 8 \pm 2.4$ s^{-1} and $k_{ss,ATP} = 0.8$ s^{-1} and were overlayed with the experimental data from Figure 7, demonstrating consistency with the proposed sequential mechanism.

occupancy activates ATP hydrolysis at the high-affinity sites. Hydrolysis of ATP at the low-affinity sites occurs thereafter. On the basis of this model, the first turnover of ATP hydrolysis, which occurs at the high-affinity sites, is dependent on the binding of ATP to the low-affinity sites and a 50% burst in ATP hydrolysis is anticipated in the burst phase of the acid-quench experiment as shown in Figures 8B and 10. However, when chased with unlabeled ATP, the radiolabeled ATP bound to the low-affinity sites will eventually hydrolyze ATP to yield a full burst in ADP formation (Figure 10). Because initial ATP hydrolysis occurs at the high-affinity sites, the burst amplitudes but not the burst rates are dependent on ATP binding to the low-affinity sites (parts B and C of Figure 8). Because peptide hydrolysis is coupled with a step after ATP hydrolysis, the binding of ATP to the low-affinity sites therefore indirectly activates the peptidase activity by stimulating ATP hydrolysis. The triphasic ATPase time courses together with the half-site reactivity in ATP hydrolysis are similar to the ATPase activity of yeast topoisomerase in which its sequential ATPase mechanism contains a burst phase and two slow steps of comparable magnitudes (*27*). It is possible that Lon adopts a similar mechanism in coupling ATPase activity to activate peptide cleavage. To further evaluate this hypothesis, we fit the averaged time courses of the acid-quenched ATPase data (from 5 to 100 μM ATP) collectively to the kinetic mechanism shown in Scheme 1 by regression analysis using FitSim (*28*−*30*) or KinFitSim (*31*). This minimal mechanism features the sequential ATPase mechanism deduced based upon the data analyses presented above and assumes that one of the product-release steps limits enzyme turnover. In addition, the concentration of enzyme used for the fitting process was varied at the respective ATP concentration based upon the data reported in Figure 8B. The two k_{on} and k_{off} for ATP binding are estimated from the two ATP affinities of Lon [<1 and 10 μM, respectively (*19*)]. Because the kinetics of product release are yet to be determined, the rate constants associated with events after steady-state turnover are at present hypothetical. Fitting the data to this mechanism yielded a pre-steady-state burst rate constant for ATP hydrolysis of 8 ± 2.4 sec^{-1} and a steady-state turnover of 4 ± 0.34 μM/sec (Figure 11), which, upon division by the 5 μM Lon monomer present in the reaction, yielded the steady-state turnover number for ATP hydrolysis of 0.8 sec^{-1}. These values are in accordance with the maximum k_{burst} of 11.3 ± 3.3 s^{-1} and $k_{cat,ATP}$ of 1.4 ± 0.1 s^{-1} determined by analyzing the pre-steady-state and steady-state time course of ATP hydrolysis separately as described above (Table 2). While the ATPase time courses presented in this study could be consistent with a sequential reaction mechanism of Lon, these experiments alone cannot conclusively determine this mechanism. Therefore, additional pre-steady-state kinetic characterizations are currently underway to further investigate the ATPase reaction mechanism of Lon in more detail.

The ATPase mechanism proposed in this study predicts that communication between the two classes of ATPase sites contribute significantly to peptide cleavage. This proposal is supported by the observation that both the ATPase and peptidase sites display the same level of positive cooperativity in the binding and hydrolysis of substrates. We observe that the k_{lag} as well as the observed steady-state rate constant ($k_{ss,S3}$) values of peptide cleavage exhibit sigmoidal dependency on S3 concentrations with a Hill coefficient (n) ranging from 1.22 to 1.7 (Table 1). Moreover, both the steady-state turnover number as well as the burst amplitude of ATP hydrolysis determined at saturating S2 and varying ATP concentrations also exhibit sigmoidal kinetics. Assuming that *E. coli* Lon is a hexamer (*14*), the maximum n value would be 6, and thus, an n value of ~1.6 measured here either suggests slight positive cooperativity among the six Lon subunits or the communication between the two classes of ATPase sites with a maximum of $n = 2$. While the extent of subunit communication cannot be defined in this study, our results clearly reveal that interactions among the subunits in Lon affect the ATPase and peptidase activities of the enzyme.

Because ATP hydrolysis does occur before S3 cleavage, we propose that nucleotide hydrolysis generates an enzyme form that subsequently cleaves S3. Lon exhibits high sequence and structural homology with the heterosubunit ATP-dependent proteases, such as HslUV, which utilizes ATP hydrolysis to deliver unfolded polypeptide substrates to the proteolytic site (*14*, *15*, *17*, *32*−*34*). This similarity suggests that ATP consumption serves a similar function in Lon. Previously, we employed steady-state kinetics and product inhibition studies to construct a kinetic model to account for the observed "ATPase-dependent" S3 cleavage reaction by Lon (*11*). Because the identities of different enzyme intermediates existing along the peptidase reaction pathway are not defined, we cannot fit the time courses of the peptidase reactions to a defined kinetic mechanism as in the case for the ATPase reaction. However, a simplified version of this model showing the microscopic events associated with S3 cleavage is provided in Scheme 2. This model proposes that ATP hydrolysis facilitates the delivery of S3 to the peptidase site of Lon and the exchange of ADP with ATP in step 3 is rate-limiting. In the presence of excess S3, the peptide binds to an allosteric site in Lon to promote the exchange of ADP with ATP, thereby increasing the catalytic turnover of ATP hydrolysis. The data obtained in this study support this proposed model by revealing that ATP hydrolysis precedes peptide bond cleavage. The hydrolysis of ATP (step 2) occurs with an apparent rate constant of ~11 s^{-1} (Table 2) to generate an active enzyme form "F"

Scheme 2

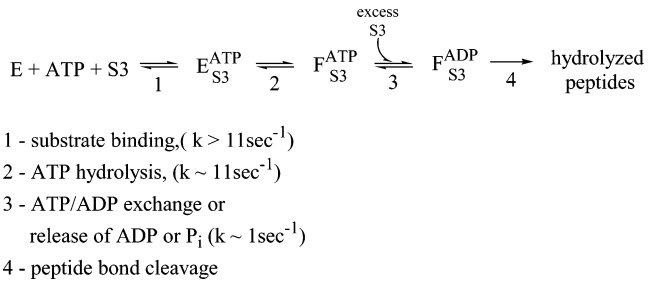

that, upon the exchange of ADP with ATP, cleaves S3 (step 3). We tentatively assign step 3 as the slow step because ADP inhibits S3 cleavage and its slow release from Lon would be consistent with the detection of burst kinetics in ATP hydrolysis (Figure 5). If F/ATP/S3 is the enzyme form that catalyzes peptide bond cleavage and subsequent steps associated with S3 cleavage are fast, then the kinetics of S3 cleavage will exhibit a lag whose duration depends on the kinetics of ADP and/or P_i dissociation. Because the lag rate constant for S3 cleavage is ~1 s^{-1} (Table 1) and the k_{cat} of ATP hydrolysis is ~1.2 s^{-1} (Table 2), it is conceivable that such coordination between the two hydrolytic events occurs in the first turnover of S3 cleavage. However, it is also possible that the k_{cat} of ATP hydrolysis and the k_{lag} of S3 cleavage are coordinated successively in the reaction pathway of Lon. In this case, both steps contribute sequentially to limit the turnover of peptide hydrolysis. The data presented in this study cannot distinguish between these two possibilities, and further kinetic characterization is needed to further delineate this mechanism.

In addition to peptide translocation, the ATPase activity of Lon could also be used to facilitate other kinetic events prior to peptide cleavage. For example, because Lon functions as an oligomer, ATP hydrolysis may be used to promote enzyme oligomerization or to induce a conformational change in the oligomer that facilitates peptide cleavage. The kinetic data presented in this study cannot disprove these possibilities because these events occur before S3 cleavage. However, studies performed on the oligomerization of Lon homologues (*3*, *35*, *36*) thus far have revealed that the enzyme oligomerization is independent of nucleotide, thereby excluding the possibility that ATP consumption is coupled to enzyme oligomerization. However, unpublished data (Lee and Burke) suggest that the oligomerization of Lon is a reversible process that is sensitive to reaction conditions. As such, studies are currently being conducted to evaluate the effect of ATP on the oligomeric state of Lon under the reaction conditions used in these studies.

ACKNOWLEDGMENT

We thank Hilary Frase and Joyce Jentoft for their assistance in preparing this manuscript.

REFERENCES

1. Chung, C. H., and Goldberg, A. L. (1981) The product of the lon (capR) gene in *Escherichia coli* is the ATP-dependent protease, protease La, *Proc. Natl. Acad. Sci. U.S.A. 78*, 4931−4935.
2. Gottesman, S., Gottesman, M. E., Shaw, J. E., and Pearson, M. L. (1981) Protein degradation by protease La from *Escherichia coli*, *J. Cell. Biochem. 32*.
3. Goldberg, A. L., Moerschell, R. P., Chung, C. H., and Maurizi, M. R. (1994) ATP-dependent protease La (lon) from *Escherichia coli*, *Methods Enzymol. 244*, 350−375.
4. Gottesman, S., and Maurizi, M. (1992) Regulation by proteolysis: Enegry-dependent proteases and their targets, *Microbiol. Rev. 56*, 592−621.
5. Gottesman, S. (1996) Proteases and their targets in *Escherichia coli*, *Annu. Rev. Genet. 30*, 465−506.
6. Maurizi, M. R. (1992) Proteases and protein degradation in *Escherichia coli*, *Experientia 48*, 178−201.
7. Charette, M. F., Henderson, G. W., Doane, L. L., and Markovitz, A. (1984) DNA-stimulated ATPase activity on the lon (CapR) protein, *J. Bacteriol. 158*, 195−201.
8. Schoemaker, J. M., Gayda, R. C., and Markovitz, A. (1984) Regulation of cell division in *Escherichia coli*: SOS induction and cellular location of the sulA protein, a key to lon-associated filamentation and death, *J. Bacteriol. 158*, 551−561.
9. Goldberg, A. L., and Waxman, L. (1985) The role of ATP hydrolysis in the breakdown of proteins and peptides by protease La from *Escherichia coli*, *J. Biol. Chem. 260*, 12029−12034.
10. Goff, S. A., and Goldberg, A. L. (1985) Production of abnormal proteins in *E. coli* stimulates transcription of lon and other heat shock genes, *Cell 41*, 587−595.
11. Thomas-Wohlever, J., and Lee, I. (2002) Kinetic characterization of the peptidase activity of *Escherichia coli* Lon reveals the mechanistic similarities in ATP-dependent hydrolysis of peptide and protein substrates, *Biochemistry 41*, 9418−9425.
12. Chin, D. T., Goff, S. A., Webster, T., Smith, T., and Goldberg, A. L. (1988) Sequence of the lon gene in *Escherichia coli*. A heat-shock gene which encodes the ATP-dependent protease La, *J. Biol. Chem. 263*, 11718−11728.
13. Amerik, A., Chistiakov, L. G., Ostroumova, N. I., Gurevich, A. I., and Antonov, V. K. (1988) Cloning, expression, and structure of the functionally active shortened lon gene in *Escherichia coli*, *Bioorg. Khim. 14*, 408−411.
14. Botos, I., Melnikov, E. E., Cherry, S., Tropea, J. E., Khalatova, A. G., Rasulova, F., Dauter, Z., Maurizi, M. R., Rotanova, T. V., Wlodawer, A., and Gustchina, A. (2004) The catalytic domain of *Escherichia coli* Lon protease has a unique fold and a Ser-Lys dyad in the active site, *J. Biol. Chem. 279*, 8140−8148.
15. Botos, I., Melnikov, E. E., Cherry, S., Tropea, J. E., Khalatova, A. G., Rasulova, F., Dauter, Z., Maurizi, M. R., Rotanova, T. V., Wlodawer, A., and Gustchina, A. (2004) Crystal structure of the AAA+ α domain of *E. coli* Lon protease at 1.9 Å resolution, *J. Struct. Biol. 146*, 113−122.
16. Sousa, M. C., Trame, C. B., Tsuruta, H., Wilbanks, S. M., Reddy, V. S., and McKay, D. B. (2000) Crystal and solution structures of an HslUV protease−chaperone complex, *Cell 103*, 633−643.
17. Wang, J., Song, J. J., Seong, I. S., Franklin, M. C., Kamtekar, S., Eom, S. H., and Chung, C. H. (2001) Nucleotide-dependent conformational changes in a protease-associated ATPase HsIU, *Structure 9*, 1107−1116.
18. Waxman, L., and Goldberg, A. L. (1982) Protease La from *Escherichia coli* hydrolyzes ATP and proteins in a linked fashion, *Proc. Natl. Acad. Sci. U.S.A. 79*, 4883−4887.
19. Menon, A. S., and Goldberg, A. L. (1987) Binding of nucleotides to the ATP-dependent protease La from *Escherichia coli*, *J. Biol. Chem. 262*, 14921−14928.
20. Menon, A. S., Waxman, L., and Goldberg, A. L. (1987) The energy utilized in protein breakdown by the ATP-dependent protease (La) from *Escherichia coli*, *J. Biol. Chem. 262*, 722−726.
21. Menon, A. S., and Goldberg, A. L. (1987) Protein substrates activate the ATP-dependent protease La by promoting nucleotide binding and release of bound ADP, *J. Biol. Chem. 262*, 14929−14934.
22. Lee, I., and Berdis, A. J. (2001) Adenosine triphosphate-dependent degradation of a fluorescent λ N substrate mimic by Lon protease, *Anal. Biochem. 291*, 74−83.
23. Patterson, J., Vineyard, D., Thomas-Wohlever, J., Behshad, R., Burke, M., and Lee, I. (2004) Correlation of an adenine-specific conformational change with the ATP-dependent peptidase activity of *Escherichia coli* Lon, *Biochemistry 43*, 7432−7442.
24. Gilbert, S. P., and Mackey, A. T. (2000) Kinetics: A tool to study molecular motors, *Methods 22*, 337−354.
25. Frieden, C. (1979) Slow transitions and hysteretic behavior in enzymes, *Annu. Rev. Biochem. 48*, 471−489.
26. Frieden, C. (1970) Kinetic aspects of regulation of metabolic processes. The hysteretic enzyme concept, *J. Biol. Chem. 245*, 5788−5799.

27. Harkins, T. T., and Lindsley, J. E. (1998) Pre-steady-state analysis of ATP hydrolysis by *Saccharomyces cerevisiae* DNA topoisomerase II. 2. Kinetic mechanism for the sequential hydrolysis of two ATP, *Biochemistry 37*, 7292−7298.
28. Zimmerle, C. T., and Frieden, C. (1989) Analysis of progress curves by simulations generated by numerical integration, *Biochem. J. 258*, 381−387.
29. Frieden, C. (1994) Analysis of kinetic data: Practical applications of computer simulation and fitting programs, *Methods Enzymol. 240*, 311−322.
30. Dang, Q., and Frieden, C. (1997) New PC versions of the kinetic-simulation and fitting programs, KINSIM and FITSIM, *Trends Biochem. Sci. 22*, 317.
31. Svir, I. B., Klymenko, A. V., and Platz, M. S. (2002) KinFitSim−A software to fit kinetic data to a user selected mechanism, *Comput. Chem. 26*, 379−386.
32. Neuwald, A. F., Aravind, L., Spouge, J. L., and Koonin, E. V. (1999) AAA+: A class of chaperone-like ATPases associated with the assembly, operation, and disassembly of protein complexes, *Genome Res. 9*, 27−43.
33. Ogura, T., and Wilkinson, A. J. (2001) AAA+ superfamily ATPases: Common structure−diverse function, *Genes Cells 6*, 575−597.
34. Wang, J., Song, J. J., Franklin, M. C., Kamtekar, S., Im, Y. J., Rho, S. H., Seong, I. S., Lee, C. S., Chung, C. H., and Eom, S. H. (2001) Crystal structures of the HslVU peptidase−ATPase complex reveal an ATP-dependent proteolysis mechanism, *Structure 9*, 177−184.
35. Stahlberg, H., Kutejova, E., Suda, K., Wolpensinger, B., Lustig, A., Schatz, G., Engel, A., and Suzuki, C. K. (1999) Mitochondrial Lon of *Saccharomyces cerevisiae* is a ring-shaped protease with seven flexible subunits, *Proc. Natl. Acad. Sci. U.S.A. 96*, 6787−6790.
36. Rudyak, S. G., Brenowitz, M., and Shrader, T. E. (2001) Mg^{2+}-linked oligomerization modulates the catalytic activity of the Lon (La) protease from *Mycobacterium smegmatis*, *Biochemistry 40*, 9317−9323.

BI048618Z